

실란처리가 치과 수복물용 고분자 침투 세라믹의 기계적 물성에 미치는 영향

신지연 · 이득용[†] · 송요승* · 김배연**

대림대학교 의공융합과, *한국항공대학교 재료공학과, **인천대학교 신소재공학과
(2018년 4월 24일 접수, 2018년 5월 23일 수정, 2018년 7월 4일 채택)

Effect of Silane Treatment on Mechanical Properties of Polymer-infiltrated Ceramic Dental Materials

Ji-Yeon Shin, Deuk Yong Lee[†], Yo-Seung Song*, and Bae-Yeon Kim**

Department of Biomedical Engineering, Daelim University, Anyang 13916, Korea

*Department of Materials Engineering, Korea Aerospace University, Goyang 10540, Korea

**Department of Materials Science and Engineering, Incheon National University, Incheon 22012, Korea

(Received April 24, 2018; Revised May 23, 2018; Accepted July 4, 2018)

초록: 1~20 wt% 실란 처리한 다공성 세라믹 전성형체에 단량체를 침투하고 중합반응을 거쳐 고분자 침투 세라믹 (PIC)을 제조하여 실란 농도별 PIC 기계적 물성을 조사하였다. 최적의 경도(99.5 Hv), 강도(271±10 MPa), 파괴인성(3.74±0.11 MPa·m^{1/2})이 14 wt% 실란 처리한 PIC에서 관찰되었다. 하지만, 실란 농도가 15% 이상이 되면 기계적 물성은 감소하였다. 파괴거동은 실란 농도가 증가함에 따라 입계파괴에서 입내파괴로 변화하였다. 대부분의 균열 에너지는 세라믹 입자를 통과하면서 소진되었다. PIC는 실란 농도에 관계없이 세포 용해 또는 독성을 일으키지 않아 임상적으로 치과용 수복물에 적합하였다.

Abstract: Polymer-infiltrated ceramics (PICs) were prepared by monomer infiltration into porous ceramic preforms and subsequent polymerization by varying the silane concentration in the range of 1 to 20 wt% to investigate the effect of silane concentration on mechanical properties of the PICs. The optimized hardness, the strength and the fracture toughness of 99.5 Hv, 271±10 MPa and 3.74±0.11 MPa·m^{1/2} were observed for the PICs having a silane concentration of 14%. However, they started to decrease when the silane content was raised more than 15%. The fracture mode was changed from intergranular to transgranular fracture across the ceramic particles with increasing the silane content. Most of the crack energy was dissipated by passing through the ceramic particles rather than through the polymer. The PICs exhibited no evidence of causing cell lysis or toxicity regardless of silane concentration, implying that the PICs are clinically suitable for use as dental restorations.

Keywords: polymer-infiltrated ceramics, silane-treatment, mechanical properties, cytotoxicity.

Introduction

Although tougher ceramics have been used in dentistry, all ceramic systems limit a widespread use due to the brittleness and higher hardness.¹⁻⁸ It is necessary to develop a dental material with similar mechanical properties to that of natural human enamel and dentin. Nowadays, the development of dental esthetic materials has switched to more polymer-based resin composites.⁸ Ceramics and polymers are highly suitable for the

synthesis of composites with tailored mechanical properties due to their synergic combination of excellent strength and flexibility, which can be used for dental restorations.⁸⁻¹¹ Unlike conventional processing of dispersion of ceramic particles in a polymer matrix, a stabilized interpenetrating network materials can be achieved by infiltration of monomers in a porous ceramic matrix, followed by polymerization. By replacing loose ceramic particles in the polymer matrix by a stable ceramic matrix, higher strength, elastic modulus, toughness, and better wear resistance are possible.⁸⁻¹³

The ceramic inlays can be fabricated by using a CAD/CAM machine at the chairside in the dental surgery. Especially, the prefabricated leucite-reinforced glass ceramic blocks were

[†]To whom correspondence should be addressed.
dylee@daelim.ac.kr, ORCID[®]0000-0003-1674-412X
©2018 The Polymer Society of Korea. All rights reserved.

available for milling using a CAD/CAM machine because of easy manipulation, excellent fit, and aesthetics.¹³ In addition, the same chemical composition of porcelain and glass ceramic made it possible to perform conventional finishing processes such as add-ons, staining and glazing. However, their mechanical properties of the glass ceramics were not suitable for use even in a single crown.^{8,13} In the present study, the polymer-infiltrated ceramic composites (PICs) are prepared to improve the mechanical properties by modifying the ceramic matrix surface with a silane coupling agent, (3-(trimethoxysilyl)propyl methacrylate), having the same active function as the resin before the monomer infiltration into the porous ceramic matrix to improve the interface strength between the organic polymer and the inorganic ceramic.^{9,14} The silane coupling agents are adhesion promoters to chemically unify dissimilar materials used in dentistry.¹⁴ The PIC, a hybrid block for milling, can be used as the material of choice for dental inlay materials. Mechanical properties, cytotoxicity and cell proliferation of the PICs were examined.

Experimental

Materials. Ceramic (leucite) preforms (11×13×21 mm³) were kindly provided by Hass Co., Korea. A silane coupling agent, 3-(trimethoxysilyl)propyl methacrylate (TMPMA, CH₂=C(CH₃)CO₂(CH₂)₃Si(OCH₃)₃, 98%) was purchased from Sigma-Aldrich, Germany. Monomers, triethylene glycol dimethacrylate (TEGDMA, CH₂=C(CH₃)COO(CH₂CH₂O)₃COC(CH₃)=CH₂, 95%) and diurethane dimethacrylate (UDMA, R'CH₂[C(CH₃)(R)CH₂]₂CH₂R', ≥97%) were also purchased from Sigma-Aldrich. Benzoyl peroxide (BPO, C₄H₁₀O₄, Daejung Chemicals & Metals Co., Ltd., Korea) was used as a heat sensitive polymerization initiator. Acetic acid (CH₃COOH, 99.5%), NaOH (98%), and ethanol (CH₃CH₂OH, 99.9%) were obtained from Samchun Pure Chemical Company (Korea). All chemicals were used as received without any further purification.

Synthesis of PIC. Prior to the silane treatment, the ceramic preforms were immersed in 0.1 M NaOH for 1 h, followed by cleaning with distilled water. To obtain a good adhesion between ceramic and polymer, the preforms were modified by a silane coupling agent (TMPMA) before the monomer was infiltrated. The surface modification was performed by immersing the ceramic preforms into the silane solution (pH 4) and stirring overnight.⁹ The silane was firstly activated by acetic acid to form silanol (-SiOH) before they can bond to the ceramic

matrix, which was fast and reversible protonation of the alkoxy group. The bond is then cleaved between the alcohol and the silicon atom, leading to the hydrolysis process until all alkoxy groups were substituted.¹⁴ The silane-treated preforms were cleaned by using ethanol and distilled water to eliminate the unreacted residual silane. The preforms were then dried for 12 h at 100 °C in a vacuum of 20 torr.

Monomers, TEGDMA and UDMA, were prepared in a 1:1 mol ratio. In addition, 0.3% of BPO, the polymerization initiator, was added and stirred at 45 °C. The porosity of the preforms were examined by using a Mercury porosimeter (AutoPoreIV, Micromeritics Instrument Corp., USA). The infiltration of the preforms was achieved with a two-step dip coating process.⁹ The temperature of the pressure chamber was raised to 45 °C to reduce the viscosity of the monomer mixture. The monomer mixture was then fed into the chamber twice. The first injection is such that the ceramic preform was half submerged. To obtain a complete infiltration without trapped gases, the preforms were stored in an infiltration chamber for 3 h under vacuum. Later, the monomer was injected into the chamber to soak the entire ceramic preform. The specimen was then stored for 1 h in air. After a complete air removal of the monomer mixture, nitrogen gas was injected into the pressure chamber (1.6 MPa) to obtain the complete monomer-soaked ceramics through the capillary forces. The monomers inside the ceramic matrix were then polymerized for 2 h at 100 °C in the pressure chamber. A volume reduction of approximately 10% may occur during the conversion from monomer to polymer.⁹ The polymerization shrinkage is likely to cause the shrinkage-induced defects. To fill up the defects with liquid monomer, N₂ gas was supplied to the vacuum chamber. After the polymerization process, the specimens were removed from the chamber, cut in discs, and the surfaces of all specimens were polished. The silane-treated preforms and PICs were evaluated with the aid of an XRD (X-ray diffraction, Mac Science, KFX-987228-SE, Japan), and a SEM (scanning electron microscope, Hitachi S-3000H, Japan). The XRD analysis was carried out with a scan speed of 5° 2θ/min at a 2θ range of 10° to 80°.

Characterization. The specimens were initially ground and polished to a 1 μm diamond finish. The strength of the PICs was evaluated by a flat-on-three-ball biaxial flexure testing at a crosshead speed of 1 mm/min (Model 5564, Instron, USA) according to ASTM Standard F394-78.³⁻⁷ Biaxial flexure disks with a diameter of 12 mm were initially ground on both sides to a nominal thickness of 1.2 mm. After a Vickers indentation,

the lengths of the indenter (a) and the cracks (c) were measured using a Vickers hardness tester (AVK-C2, Akashi, Japan) on the surface of the polished specimens under the load conditions appropriate to the specimens. Then, the hardness (H) and the fracture toughness (K_{Ic}) were determined. The fracture toughness was measured by the equation of $K_{Ic} = 0.203 \times (c/a)^{3/2} \times H \times a^{1/2}$, given by Evans and Charles.¹⁵

Cytotoxicity. The extract test method was conducted on the PICs to evaluate the potential of cytotoxicity on the base of the International Organization for Standardization (ISO 10993-5).¹⁶⁻¹⁹ The PICs were extracted aseptically in single strength Minimum Essential Medium (1X MEM, Dulbecco's Modified Eagles's Medium (Gibco) with 10% fetal bovine serum (Gibco) and 1% penicillin-streptomycin) with serum. The ratio of the PICs to extraction vehicle was 0.2 g/mL. The 96-well plate was incubated at a temperature of 37 °C in a 5% CO₂ atmosphere. The test extracts were maintained in an incubator for 24 h. The test extracts were placed onto three separate confluent monolayers of L-929 (NCTC Clone 929, ATCC, USA) mouse fibroblast cells propagated in 5% CO₂. For this test, confluent monolayer cells were trypsinized and seeded in 10 cm² wells (35 mm dishes) with a micropipette. Simultaneously, triplicates of reagent control, negative control (high density polyethylene film, RM-C), and positive control (polyurethane film, RM-A) were placed onto the confluent L-929 monolayers. All monolayers were incubated for 48 h at 37 °C in the presence of 5% CO₂. After incubation, the morphological change of the cell was examined to assess the biological reaction by using the inverted microscope (TS100-F, Nikon, Japan) and the iMark microplate absorbance spectrophotometer (Bio-Rad, USA).¹⁶ Water-soluble tetrazolium salts (WSTs) are a series of other water-soluble dyes for MTT assays, which can provide different absorption spectra of the formed formazans. EZ-cytox yields a water-soluble formazan, which can be read directly. The absorbance of the colored solution is quantified by measuring at a wavelength of 415 nm with the microplate absorbance spectrophotometer.¹⁶⁻¹⁹ The value of untreated cell (control sample, only cultured with culture medium) was set as 100% and those of the treated cells were expressed as the percentage of the control sample.

Cell Proliferation. Cell counting kit-8 (CCK-8, Dojindo Molecular Technologies, Inc., Japan) was used for the assay of cell proliferation. CCK-8, being nonradioactive, allows sensitive colorimetric assays for the determination of the number of viable cells in cell proliferation.¹⁵ WST is reduced by dehydrogenases in cells to give an orange colored product (for-

mazan), which is soluble in the tissue culture medium. The amount of the formazan dye generated by dehydrogenases in cells is directly proportional to the number of living cells. The 96-well plate containing 100 μL of cell suspension (5×10^3 cells/well) was incubated for 24 h at a temperature of 37 °C in a 5% CO₂ atmosphere. The test extracts (10 μL) were added to the plate and maintained for an appropriate length of time (6, 12, 24, 48 h) in an incubator. After adding 10 μL of CCK-8 solution to each well of the plate, the plate was incubated for 2 h. Then, the absorbance of the colored solution is quantified by measuring at a wavelength of 450 nm with the microplate absorbance spectrophotometer.¹⁶

Results and Discussion

The surface of the ceramic (leucite, K[AlSi₂O₆]) preforms treated with 0.1 M NaOH (-OH bonding) was modified with a silane agent before the monomers were infiltrated. The TMPMA is a silane coupling agent whose molecule contains acrylate functional group (CH₂=CHCOO-) that bonds with both ceramic and polymer materials, as depicted in Figure 1. XRD results revealed that the ceramic (leucite) peaks were

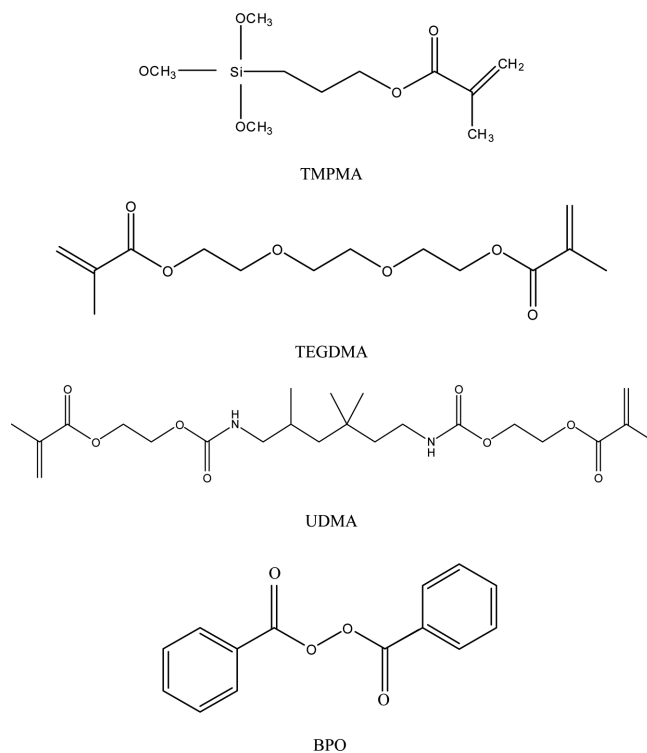


Figure 1. Chemical structures of TMPMA, TEGDMA, UDMA, and BPO, respectively.

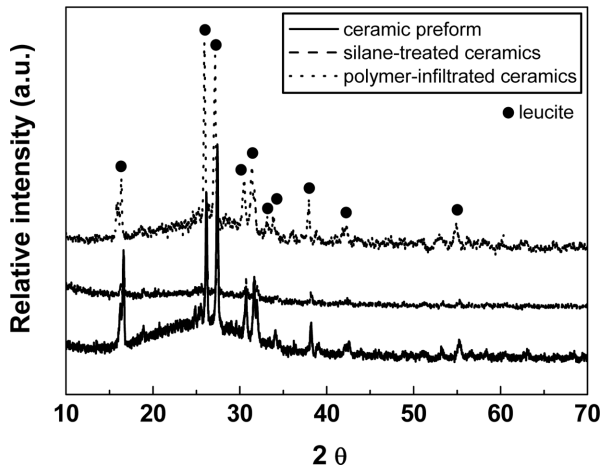


Figure 2. XRD patterns of the leucite preforms (before and after silane treatment) and the polymer-infiltrated leucite.

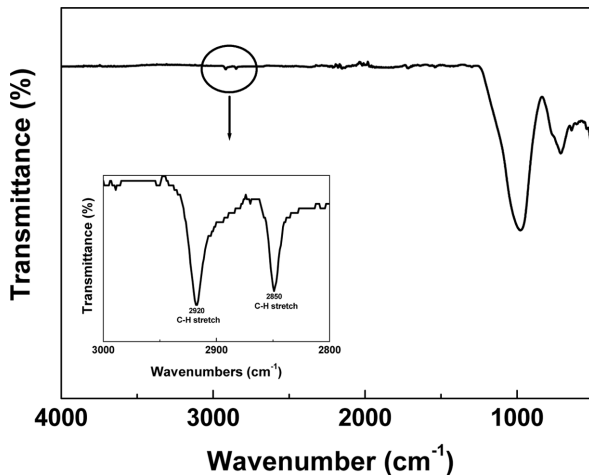


Figure 3. FTIR spectra of the silane-treated ceramic preforms.

almost identical regardless of the silane treatment, as shown in Figure 2. Monomers with acrylate groups at the end of the monomer were used for polymerization by using a heat-sensitive BPO having an ether bond (-O-) as a polymerization initiator. The BPO radicals having a single electron with breakage of -O-O- bond due to heat became unstable and acted as ini-

tiator by easily breaking the double bonded structure (acrylate bond, C=C), resulting in a network structure connected with both ends of TEGMA and UDMA. The surface modification with TMPMA was performed to promote the adhesion between the ceramic preforms and the monomers with an aid of hydrogen bonding. The FTIR spectra of the silane treated ceramic preforms are depicted in Figure 3. The ceramic preforms exhibited characteristic silicate chain (-Si-O-Si-) absorption peaks at 985 and 710 cm^{-1} . The Si-O bond by silane treatment was not conclusive because leucite also possessed a Si-O-Si bond and an Al-O-Si bond.^{1,20} However, the peaks at 2920 and 2850 cm^{-1} in Figure 3 were identified and associated to the C-H asymmetric and symmetric stretching, suggesting the presence of alkyl group as a result of silane treatment.

The porosity of the silane-treated preforms were examined by using a Mercury porosimeter. The porosity and the average pore diameter of the ceramic preforms were $\sim 42.9 \pm 0.8\%$ and $0.53 \sim 1.1 \mu\text{m}$, respectively. As the preforms were silane-treated up to 20%, no appreciable reduction in porosity ($42.1 \pm 0.6\%$) and pore size ($0.48 \sim 0.56 \mu\text{m}$) was detected, suggesting that the pores inside the ceramic preforms were uniformly coated without blocking the pores with silane precipitates. However, the porosity of the silane-treated PIC decreased dramatically down to $\sim 1.7 \pm 0.5\%$ due to polymer infiltration into ceramic matrix.

To investigate the effect of silane concentration (1 to 20 wt%) on mechanical properties of PICs, hardness, biaxial strength and fracture toughness were examined. Optical photographs of the cross-sections of PICs are shown in Figure 4. If there is a portion that is not infiltrated, it is displayed in white. No white portion was visible in Figure 4, indicating that the PICs were fully polymer-infiltrated. Hardness was determined by placing a Vickers diamond indent of 19.6 N on the surface after polishing. Hardness increased from 85.4 to 99.5 Hv with increasing the silane concentration up to 14% and then decreased with further increasing the silane content, as depicted in Figure 5. The highest hardness (99.5 Hv) was observed for the PICs having the silane concentration of 14 wt%. After a Vickers

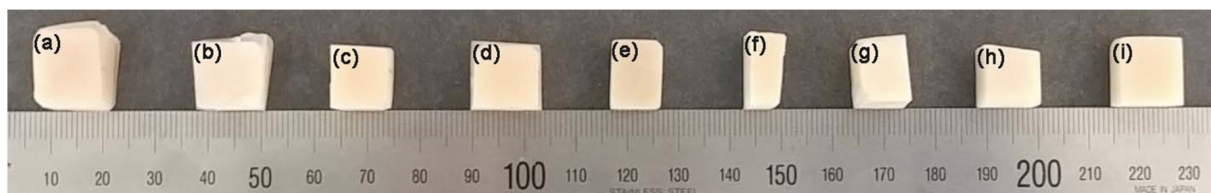


Figure 4. Optical photographs of the cross-sections of PICs as a function of silane concentration: (a) 1%; (b) 5%; (c) 10%; (d) 13%; (e) 14%; (f) 15%; (g) 16%; (h) 17%; (i) 20%, respectively.

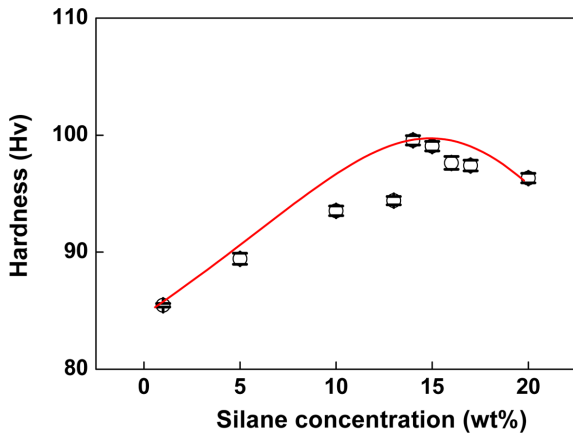


Figure 5. The variation of hardness as a function of silane concentration.

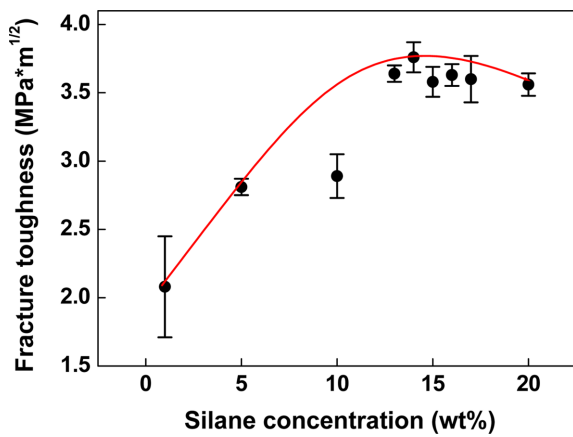


Figure 6. The variation of fracture toughness of PICs as a function of silane concentration.

indentation of 490 N, the fracture toughness was determined by the equation given by Evans and Charles.¹⁵ As the silane concentration was raised up to 14 wt%, it increased from $2.08 \pm 0.37 \text{ MPa}\cdot\text{m}^{1/2}$ to $3.74 \pm 0.11 \text{ MPa}\cdot\text{m}^{1/2}$, as displayed in Figure 6. And then it decreased to $3.56 \pm 0.08 \text{ MPa}\cdot\text{m}^{1/2}$ when the silane concentration was 20 wt% probably due to the precipitation of SiO_2 as a result of oversaturation. The variation in fracture toughness (Figure 6) showed a similar trend to that of the hardness in Figure 5. The biaxial strength of the optimized PICs was $271 \pm 10 \text{ MPa}$. The hardness, the strength and the fracture toughness of the PICs were reported to be 50~70 Hv, 100~120 MPa and $1.2 \sim 1.5 \text{ MPa}\cdot\text{m}^{1/2}$, respectively.^{13,21,22} The enhanced hardness, biaxial strength and fracture toughness of the PICs were 99.5 Hv, $271 \pm 10 \text{ MPa}$, and $3.74 \pm 0.11 \text{ MPa}\cdot\text{m}^{1/2}$, respectively. The mechanical properties of PICs were improved dramatically, suggesting that they were suitable for

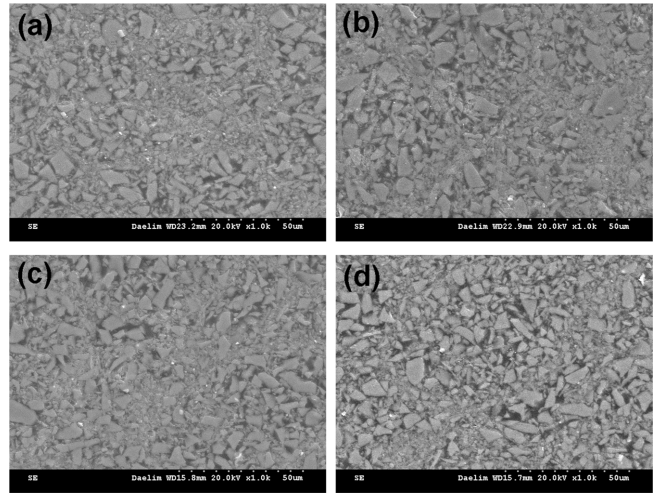


Figure 7. SEM images of the PICs as a function of the silane concentration: (a) 1%; (b) 10%; (c) 14%; (d) 20%, respectively.

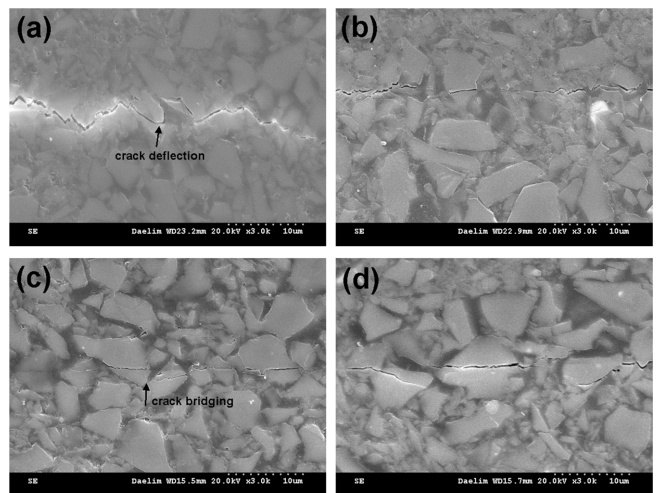


Figure 8. SEM micrographs of the indented PICs having a silane concentration of (a) 1%; (b) 10%; (c) 14%; (d) 20%, respectively.

dental inlay materials.

It is necessary that the PICs possess as high ceramic loading as possible to maintain mechanical properties. The microstructures of various PICs are shown in Figure 7. A quantitative image analysis from the micrographs by measuring the area indicated that the ceramic fractions in the PICs are 55 ± 6.9 , 65 ± 4.8 , 65 ± 7.4 and $53 \pm 2.9 \text{ vol}\%$ with increasing the silane concentration from 1%, 10%, 14% to 20%, respectively.² The results of the analysis are likely to be closely related to the hardness and the fracture toughness of the PICs. Among toughening mechanisms in ceramic composites, the mechanism that is governed by the particle spacing is the crack

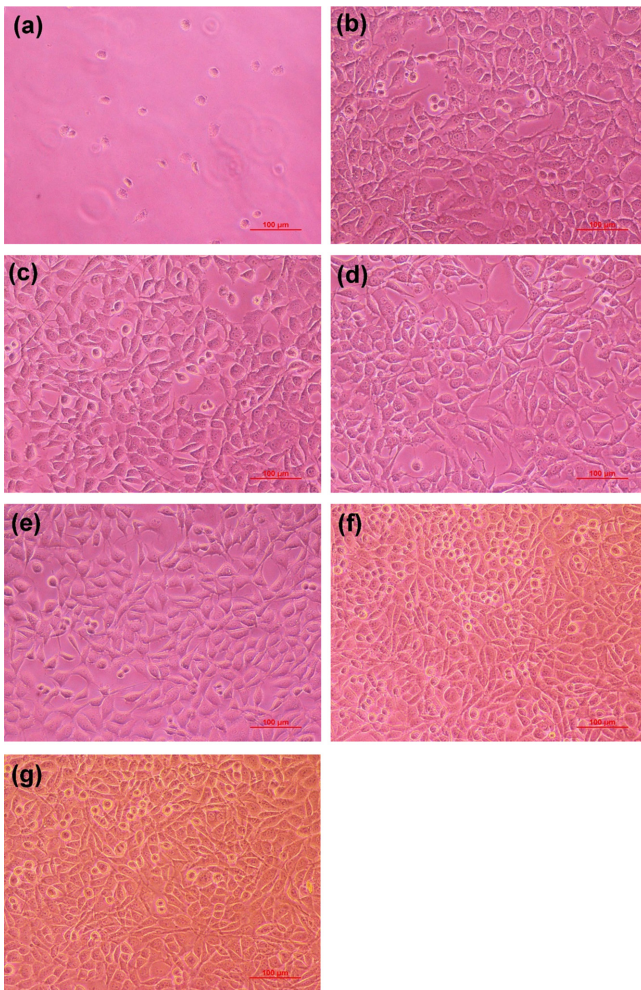


Figure 9. Photographs of cell morphologies: (a) positive control; (b) negative control and the extracts of PICs silane-treated with (c) 1%; (d) 5%; (e) 10%; (f) 14%; (g) 20%, respectively.

bowing.²⁻⁵ In this mechanism, a fracture energy must be supplied for a crack front, which is pinned at the particles, to move between the pinning positions. From the indentation cracks of the PICs, both the intergranular fracture and the partial transgranular fracture were observed for the PICs treated with 1% silane (Figure 8(a)). A zigzag pattern of intergranular crack propagation was observed. The crack paths across the polymer were likely to be ineffective in consuming the energy of the crack front. However, the transgranular fracture through the ceramic particles became dominant as the silane concentration increased. This effect was more pronounced as the silane concentration was raised up to 14%. Most of the crack energy was consumed while being used to penetrate ceramic particles, as demonstrated in Figure 8(c). Crack deflection (Figure 8(a)) and crack bridging (Figure 8(c)) were also observed in the PICs. It

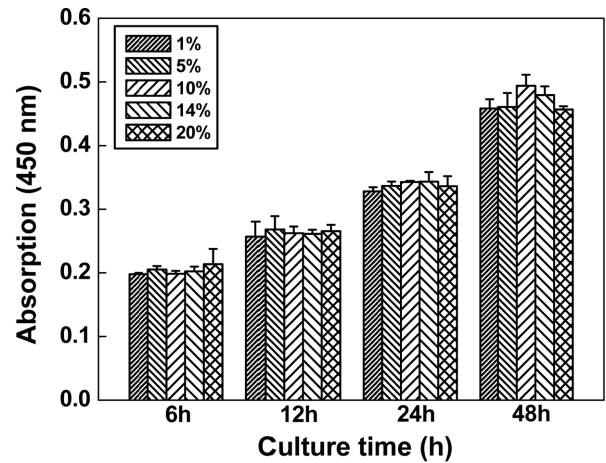


Figure 10. Proliferation of L-929 cells on various PICs.

is conceivable that higher fracture toughness may be achieved by increasing the silane concentration probably due to higher ceramic fractions and the transgranular fracture behavior.

A cytotoxicity test of the PICs treated with various silane concentration in the range of 1% to 20% determines whether the PICs will have a toxic effect on living cells. The test extracts with the PICs regardless of silane concentration showed no evidence of causing cell lysis or toxicity, as depicted in Figure 9. The PIC scaffolds silane-treated with 1, 5, 10, 14 and 20% exhibited cell viability of 102, 139, 101, 113, and 119% compared to the negative control, respectively, as measured at a wavelength of 415 nm by using the microplate absorbance spectrophotometer.¹⁶ The qualitative morphological grading of cytotoxicity of the PICs was determined to be scale 0. In addition, the cell proliferation results of silane-treated PICs (Figure 10) suggested that L-929 cells adhere well to the PICs and proliferated continuously with increasing time regardless of silane concentration. Therefore, it is conceivable that the PICs are considered to be clinically safe and effective due to the absence of cytotoxicity and excellent cell proliferation under the condition of this study.

Conclusions

The PICs were prepared by monomer infiltration into porous leucite preforms and subsequent polymerization by varying the silane concentration in the range of 1% to 20% to investigate the effect of silane concentration on mechanical properties of PICs. The monomers and the silane chemicals having the acrylate functional groups were used. The highest hardness, biaxial strength and fracture toughness of 99.5 Hv, 271±10 MPa and

3.74±0.11 MPa·m^{1/2} were found for the PICs having a silane concentration of 14%. However, they started to decrease when the silane content was more than 15% probably due to the precipitation of SiO₂. The crack paths were changed from intergranular along the leucite particles to transgranular fracture through the leucite particles with increasing the silane content. Most of the crack energy were dissipated by passing through the ceramic particles. The PICs exhibited no evidence of causing cell lysis or toxicity regardless of silane concentration, implying that the PICs are clinically safe and effective.

Acknowledgements: This research was financially supported by the Ministry of SMEs and Startups (MSS), Korea, under the “Regional Specialized Industry Development Program (R0006443)” supervised by the Korea Institute for Advancement of Technology (KIAT). Special thanks as well to Drs. Hyong Bong Lim and Sungmin Kim in Hass Corp. for providing the ceramic samples.

References

1. F. Mazzi, E. Galli, and G. Gottardi, *Am. Mineral.*, **61**, 108 (1976).
2. D. Kim, M. Lee, D. Y. Lee, and J. Han, *J. Biomed. Mater. Res. (Appl. Biomater.)*, **53**, 314 (2000).
3. D. Y. Lee, D. Kim, J. Jang, D. Choi, and S. Lee, *Mater. Lett.*, **39**, 221 (1999).
4. D. Y. Lee, D. Kim, D. Cho, and M. Lee, *Ceram. Intl.*, **24**, 461 (1998).
5. D. Y. Lee, D. Kim, and B. Kim, *J. Eur. Ceram. Soc.*, **22**, 2173 (2002).
6. D. Y. Lee, D. Kim, Y. Song, and B. Kim, *Mater. Sci. Eng. A*, **341**, 98 (2003).
7. D. Y. Lee, *J. Mater. Sci.*, **39**, 3141 (2004).
8. L. He and M. Swain, *Dental Mater.*, **27**, 527 (2011).
9. V. F. Steier, C. Koplín, and A. Kailer, *J. Mater. Sci.*, **48**, 3239 (2013).
10. L. He, D. Purton, and M. Swain, *J. Mater. Sci: Mater. Med.*, **22**, 1639 (2011).
11. J. Nguyen, V. Migonney, N. D. Ruse, and M. Sadoun, *Dental Mater.*, **28**, 529 (2012).
12. R. Prehn, F. Hauptert, and K. Friedrich, *Wear*, **259**, 693 (2005).
13. T. Miyazaki and Y. Hotta, *Aust. Dent. J.*, **56**, 97 (2011).
14. J. P. Matinlinna, C. Y. K. Lung, and J. K. H. Tsoi, *Dent. Mater.*, **34**, 13 (2018).
15. A. G. Evans and E. A. Charles, *J. Am. Ceram. Soc.*, **59**, 371 (1976).
16. B. Seol, J. Shin, G. Oh, D. Y. Lee, and M. Lee, *J. Biomed. Eng. Res.*, **38**, 248 (2017).
17. Y. Kim, I. Lee, Y. Song, M. Lee, B. Kim, N. Cho, and D. Y. Lee, *Tissue Eng. Regen. Med.*, **11**, 32 (2014).
18. Y. Kim, S. Son, C. Chun, J. Kim, D. Y. Lee, H. J. Choi, and T. Kim, *Biomed. Eng. Lett.*, **6**, 287 (2016).
19. G. Oh, J. Rho, D. Y. Lee, M. Lee, and Y. Kim, *Macromol. Res.*, **26**, 48 (2018).
20. F. Jin, H. Zhang, S. Yao, and S. Park, *Macromol. Res.*, **26**, 211 (2018).
21. W. Kim, S. Kwon, S. Chung, S. Kwon, J. Park, and W. Choi, *J. Korean Soc. Tribol. Lubr. Eng.*, **23**, 318 (2007).
22. K. D. Jandt and B. W. Sigusch, *Dent. Mater.*, **25**, 1001 (2009).